

ORIGINAL RESEARCH ARTICLE

Open Access

Characterization of the human helicotrema: implications for cochlear duct length and frequency mapping



Luke Helpard^{1*}, Hao Li^{2,3}, Helge Rask-Andersen^{2,3}, Hanif M. Ladak^{1,4,5,6} and Sumit K. Agrawal^{1,4,5,6}

Abstract

Background: Despite significant anatomical variation amongst patients, cochlear implant frequency-mapping has traditionally followed a patient-independent approach. Basilar membrane (BM) length is required for patient-specific frequency-mapping, however cochlear duct length (CDL) measurements generally extend to the apical tip of the entire cochlea or have no clearly defined end-point. By characterizing the length between the end of the BM and the apical tip of the entire cochlea (helicotrema length), current CDL models can be corrected to obtain the appropriate BM length. Synchrotron radiation phase-contrast imaging has made this analysis possible due to the soft-tissue contrast through the entire cochlear apex.

Methods: Helicotrema linear length and helicotrema angular length measurements were performed on synchrotron radiation phase-contrast imaging data of 14 cadaveric human cochleae. On a sub-set of six samples, the CDL to the apical tip of the entire cochlea (CDL_{TIP}) and the BM length (CDL_{BM}) were determined. Regression analysis was performed to assess the relationship between CDL_{TIP} and CDL_{BM} .

Results: The mean helicotrema linear length and helicotrema angular length values were 1.6 ± 0.9 mm and 67.8 ± 37.9 degrees, respectively. Regression analysis revealed the following relationship between CDL_{TIP} and CDL_{BM} : $CDL_{BM} = 0.88(CDL_{TIP}) + 3.71$ ($R^2 = 0.995$).

Conclusion: This is the first known study to characterize the length of the helicotrema in the context of CDL measurements. It was determined that the distance between the end of the BM and the tip of the entire cochlea is clinically consequential. A relationship was determined that can predict the BM length of an individual patient based on their respective CDL measured to the apical tip of the cochlea.

Keywords: Helicotrema, Helicotrema size, Cochlear duct length, Basilar membrane, Cochlear apex, Cochlear implant, Frequency mapping, Synchrotron radiation

Background

Cochlear implants (CI) consist of an electrode array that is inserted along the cochlea, with discrete contacts providing stimulus directly to the auditory nerve to produce the sensation of sound. Despite significant anatomical variation in the cochleae of patients [1–4], CI frequency-mapping has traditionally followed a patient-independent approach, which may affect patient outcomes. If the cochlear duct length (CDL) can be

determined pre-operatively, an appropriate length CI can be selected, and the pitch-map of this implant can be customized using Greenwood's equation [5] if the final electrode locations are determined through post-operative imaging. If patient-specific pitch-maps are determined, CI electrode arrays can be programmed to match the true tonotopic arrangement of an individual patients' cochlea [6, 7]. Preliminary evidence suggests that this may result in improved hearing outcomes through music appreciation, pitch-discernment, and speech perception [7, 8].

Investigators have used several manual and analytical approaches to estimate CDL on an individual level to

* Correspondence: lhelpard@uwo.ca

¹School of Biomedical Engineering, Western University, London, Ontario, Canada

Full list of author information is available at the end of the article



move towards customized CI programming [3, 9–13]. Manual methods rely on the placement of points along the entire length of the cochlea, and although this technique yields accurate results for research purposes, it is not feasible in a clinical setting [4, 11, 14, 15]. Analytical approaches, such as the *A* value technique, utilize models developed from reference cochleae and generally use a small collection of measurements to estimate CDL [10, 12, 13, 16]. To achieve clinically relevant results using either technique, anatomically accurate boundary conditions must be in place to determine the start- and end-point of the CDL measurements [17]. Although the round window (RW) has been ubiquitously used as the CDL measurement start-point, lack of visual clarity in the cochlear apex has caused ambiguity in the end-point for measurements at the cochlear apex. In addition, the cochlear apex is highly variable, and therefore many modelling techniques, such as the *A* value technique, have only been accurate up to the cochlear two-turn length [13, 16, 18]. Clinically measuring the cochlear two-turn length using the *A* value can be useful for surgical planning and specifying electrode lengths, however, the entire basilar membrane (BM) length including the apical turn is needed to utilize Greenwood's equation.

The helicotrema is the most apical portion of the cochlea and is defined as the region where the scala tympani and scala vestibuli meet at the end of the BM. The BM narrows in its most apical portion, and a visible gap can be observed in the helicotrema from the end of the BM to the apical tip of the entire cochlea [19, 20]. BM length is required for the use of Greenwood's equation, however CDL measurements often extend to the apical tip of the entire cochlea or have no clearly defined end-point [4, 14, 15]. This is because the BM is often not visible at the helicotrema, even when using high-resolution micro-CT techniques [2]. Correction factors have been proposed to relate CDL measurements at the lateral wall (LW) to those at the organ of Corti, however these only correct for the radial location of the measurement and not for the helicotrema length [13, 18]. In addition to CDL, more accurate representations of the helicotrema are required for the development of numerical models to study the biophysics of the cochlear apex [21]. Synchrotron radiation phase-contrast imaging (SR-PCI) is a novel imaging approach that yields higher soft-tissue contrast than comparable techniques such as micro-CT [18, 22, 23]. In SR-PCI data, the BM is visible and can be measured in detail through its entire length to the helicotrema. In contrast to histologic sectioning, SR-PCI allows for three-dimensional (3D) volume reconstructions and does not require sectioning, decalcification, staining, and slide mounting [22].

To our knowledge, no geometric analysis has been conducted on the helicotrema region in the context of

CDL measurements. The objective of this study was to characterize the length between the end of the BM and the tip of the cochlea using SR-PCI data of cadaveric human cochleae.

Methods

Sample preparation and scanning

All cadaveric specimens used in this study were obtained with permission from the body bequeathal program at Western University (London, ON, Canada) in accordance with the Anatomy Act of Ontario and Western's Committee for Cadaveric Use in Research (approval #19062014). The entire Western University synchrotron database was analysed, and specimens were included if they contained an intact BM throughout the entire apical turn. SR-PCI data from 14 cadaveric human cochleae were included in this study.

All samples were scanned at the Canadian Light Source Inc. (Saskatoon, SK, Canada) using the Biomedical Imaging and Therapy beamline (05ID-2). The detector had an effective pixel size of 9 μm (isotropic), and 3000 projections were acquired over 180-degrees of sample rotation. Specifications of sample preparation and of the imaging technique have been previously reported [18, 22, 23].

Helicotrema measurements

The helicotrema linear length (HLL) and helicotrema angular length (HAL) were measured on all 14 samples. HLL is defined as the linear distance (measured in mm) from the end of the BM to the apical tip of the cochlea along the LW. With the modiolus used as the axis of rotation, the HAL is defined as the angular length (measured in degrees) from the end of the BM to the apical tip of the cochlea along the LW.

To measure the HLL and HAL, fiducials were placed along the LW of the cochleae at the level of the BM in the helicotrema region using 3D Slicer (<https://www.slicer.org/>), as illustrated in Fig. 1. The start-point for the helicotrema measurements was at the end of the BM, indicated by the point where the BM was no longer visible between the osseous spiral lamina and the spiral ligament in image slices and 3D volume renderings. An example start-point for helicotrema measurements is displayed using a volume rendering in Fig. 2. The end-point for the helicotrema measurements was at the apical tip of the cochlea, indicated as the point where the LW reached its vertex and began to turn towards the modiolus (as illustrated in Fig. 1). Image slices in a plane orthogonal to the cochlear scalae path were used to place fiducials from the end of the BM to the apical tip of the cochlea. Lastly, a fiducial was placed at the estimated modiolar axis location in the same plane as the previously described set of LW fiducials.

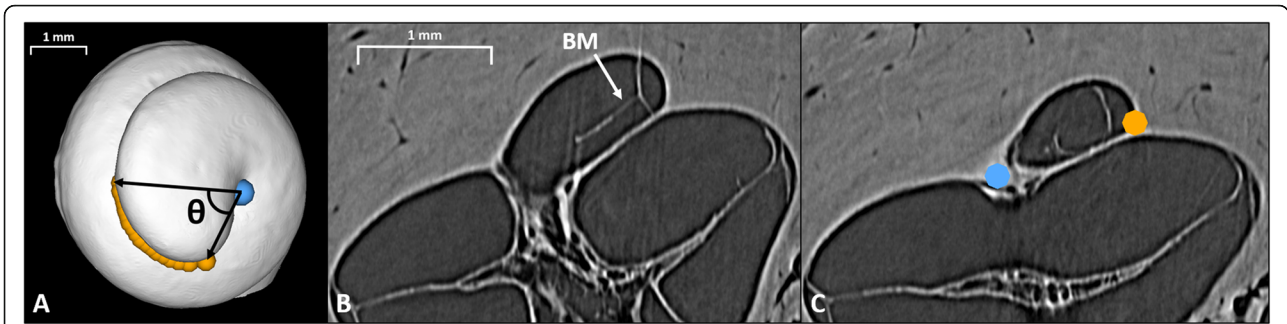


Fig. 1 **a** Illustration of the fiducials placed along the LW from the end of the BM to the apical tip of the cochlea (orange) on a 3D model of the middle and apical turns. The fiducial placed at the modiolar axis is additionally visible (blue). Θ is a visual representation of the HAL. **b** A cross-sectional image slice from SR-PCI data. The BM is visible and annotated. When progressing apically from this slice, the BM collapses towards the middle turn and quickly reaches its end-point. **c** A cross-sectional slice after the BM end-point. Fiducials are seen along the LW at the approximate level of the BM end-point (orange), and at the modiolar axis location (blue). LW denotes lateral wall; HAL denotes helicotrema angular length; SR-PCI denotes synchrotron radiation phase-contrast imaging; BM denotes basilar membrane

Image processing

Prior to the measurement of the HLL and HAL values, a custom Python (<https://www.python.org/>) script was used to process the helicotrema fiducials. To eliminate variance in the measurements due to inconsistencies in the level of fiducial placement on the LW, a plane of best fit was determined amongst the helicotrema fiducials. All fiducials were then orthogonally projected into the plane of best fit prior to measurement. The HLL was determined by summing the Euclidean distances between subsequent fiducials. The HAL was determined by first defining vectors between the modiolar axis fiducial and each helicotrema fiducial, and then summing the angles between subsequent fiducials to provide accuracy in three-dimensions.

CDL measurements

CDL values were obtained for a sub-set of six samples (out of the total 14 samples) that had visible RWs in the SR-PCI dataset. Using image slices and 3D volume renderings, fiducials were placed along the entire length of the cochleae. With the modiolar axis used as the axis of rotation and the RW serving as the 0-degree point, fiducials were placed on the LW at approximately 30-degree intervals from the RW to the apical tip of the entire cochlea. The last fiducial was placed directly at the apical tip of the cochleae. CDL values were then determined by summing the Euclidean distances between subsequent fiducials. CDL measured to the most apical tip of the entire cochlea is defined as CDL_{TIP} .

BM length was estimated in these six samples by subtracting the HLL from the respective CDL_{TIP} value. BM length is defined as CDL_{BM} .

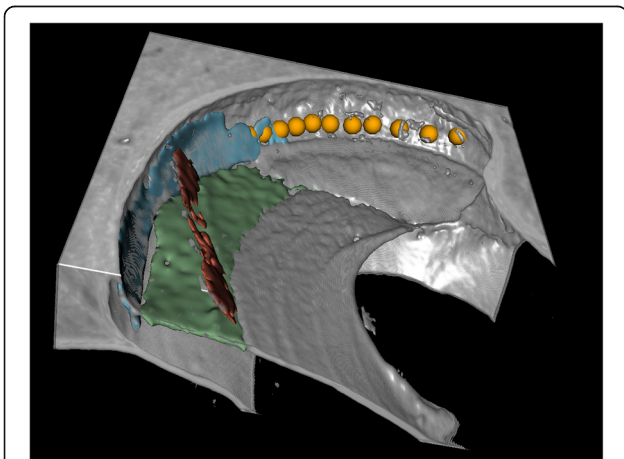


Fig. 2 3D volume rendering of the cochlear apex. Fiducials (orange) are placed along the LW from the end of the BM to the tip of the cochlea. The BM is coloured in green, Reissner's membrane is coloured in red, and the spiral ligament is coloured in blue. LW denotes lateral wall; BM denotes basilar membrane

Statistical analyses

The mean and standard deviation were calculated for the HLL and HAL values. *Mean ± standard deviation* is the convention used throughout when presenting data. Kolmogorov-Smirnov tests were conducted to assess normality in the HLL and HAL values. Confidence intervals were constructed for the HLL and HAL values at the 95% level using a *t*-distribution. Linear regression was performed to determine the relationship between HLL and HAL. This regression result was used to determine if there was a consistent morphology (helical shape) observed across samples in the helicotrema region.

The mean and standard deviation were calculated for the CDL_{TIP} and CDL_{BM} values in the sub-set of samples that had visible RW membranes. A linear regression was performed to determine the relationship between CDL_{TIP} and CDL_{BM} . This regression result was used to estimate the correction factor required to retrieve CDL_{BM} from CDL_{TIP} measurements.

All statistical analyses were completed using MATLAB (version R2018, The MathWorks, Inc., Natick, MA).

Results

HLL and HAL measurements

HLL and HAL values were measured on all 14 SR-PCI samples. The mean HLL was 1.6 ± 0.9 mm (95% confidence interval: [1.1 mm, 2.1 mm]), with minimum and maximum values of 0.7 mm and 3.8 mm, respectively. The mean HAL was 67.8 ± 37.9 degrees (95% confidence interval: [46.0 degrees, 89.7 degrees]), with minimum and maximum values of 32.4 degrees and 175.9 degrees, respectively.

Regression analysis was performed to determine the relationship between the 14 HLL and HAL measurements. Regression analysis yielded the equation, $HLL = 42.47(HAL) - 0.84$ ($R^2 = 0.933$). The determined linear function and the individual pairs of HLL and HAL values are illustrated in the plot in Fig. 3.

CDL measurements

For the six samples that had intact BMs in the apex and visible RW membranes in the SR-PCI data, the CDL_{TIP} was directly measured. The mean CDL_{TIP} value measured was 39.9 ± 1.7 mm. In these six samples, the CDL_{BM} was determined by subtracting the HLL value from the CDL_{TIP} value. The mean CDL_{BM} was determined to be 39.0 ± 1.5 mm.

Regression analysis was conducted to determine the relationship between CDL_{TIP} and CDL_{BM} in the six samples. The regression analysis yielded the equation, $CDL_{BM} = 0.88(CDL_{TIP}) + 3.71$ ($R^2 = 0.995$). The determined linear function and the individual pairs of CDL_{TIP} and CDL_{BM} values are illustrated in the plot in Fig. 4.

Discussion

CDL measurement has been a topic of growing attention in the literature, largely due to the interest in customizing CI pitch-maps for individual patients using Greenwood’s equation [5, 7, 8]. Greenwood’s equation uses an exponential function to model the frequency distribution of individual cochleae based on the respective CDL_{BM} . There has, however, been a gap between the requirement of CDL_{BM} for Greenwood’s equation and the length measurements possible using currently available imaging techniques. Due to low discernment of the BM in the apical region of the cochlea, current CDL models generally extend to the most apical point of the entire cochlea or have no clearly defined end-point in the helicotrema region.

Both direct measurements and analytical estimates are subject to error due to ambiguities in the helicotrema region. Avci et al. produced a detailed analysis of the cochlear scalae using high-resolution micro-CT [2]. Unfortunately, the authors were unable to characterize the soft-tissue beyond the middle turn, and therefore the

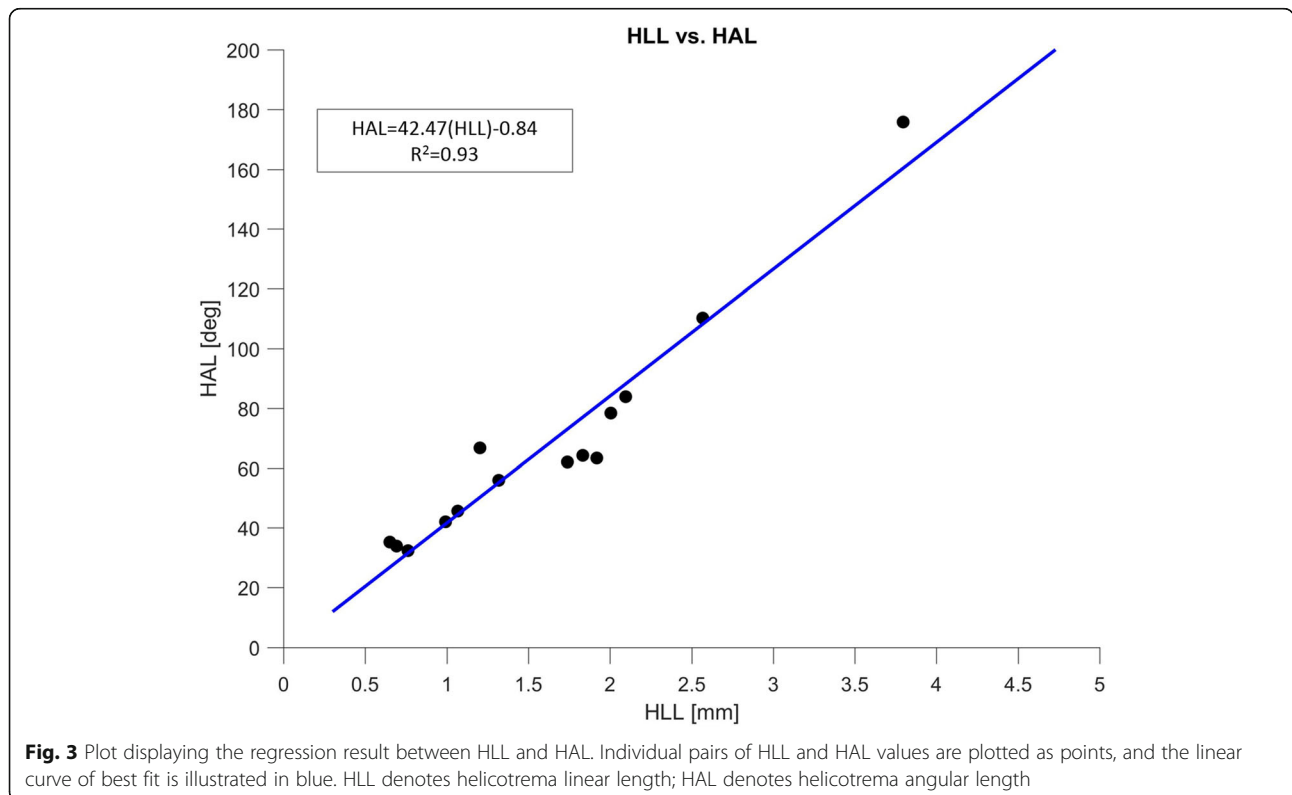
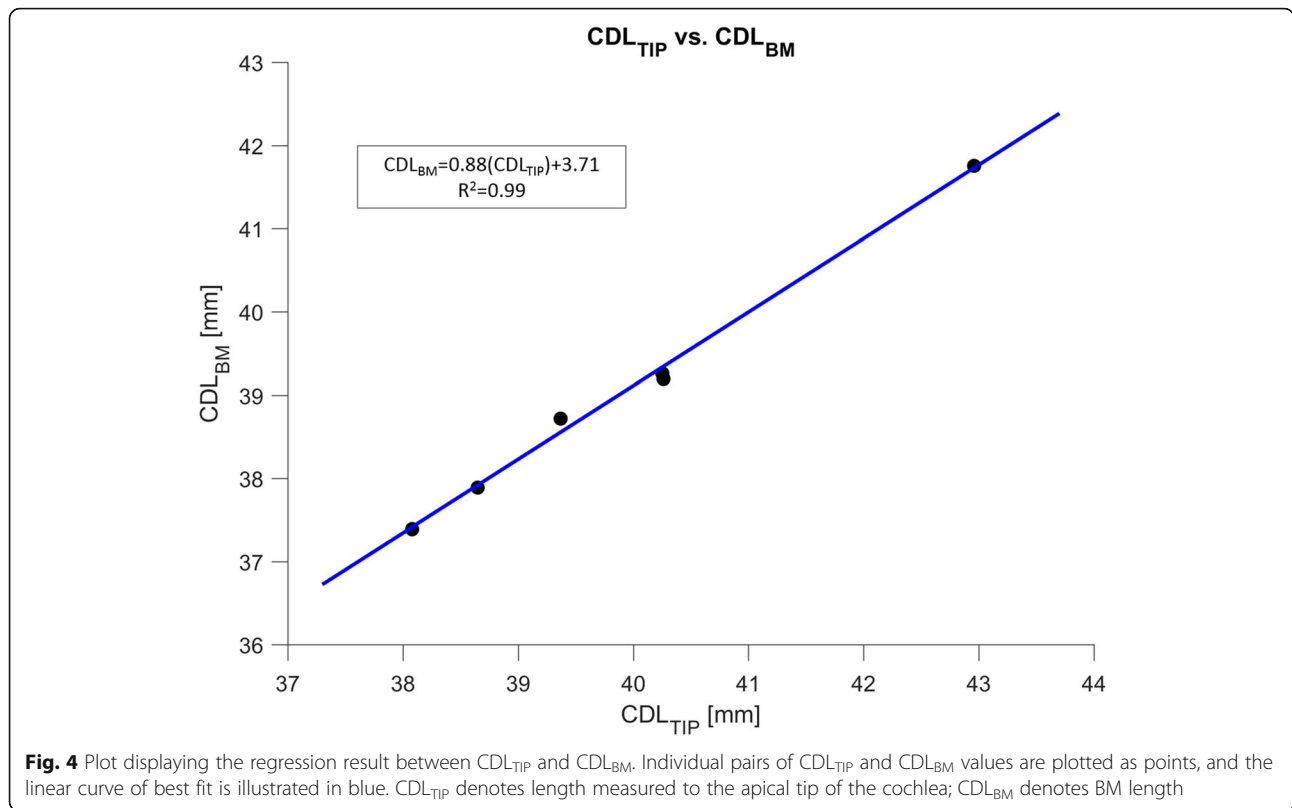


Fig. 3 Plot displaying the regression result between HLL and HAL. Individual pairs of HLL and HAL values are plotted as points, and the linear curve of best fit is illustrated in blue. HLL denotes helicotrema linear length; HAL denotes helicotrema angular length



cochlear apex was excluded from the analysis. Direct length measurement techniques, such as those proposed by Vu et al. [24], require the user to identify the exact end-point of the BM to use Greenwood’s equation. This is generally not achievable due to the lack of visualization of soft-tissue membranes in the apex. The most novel analytical estimates, such as those proposed by Schurzig et al. [25], require the user to specify an angular position for which they would like to estimate the length. In this case, the exact angular length of the BM must be identified for Greenwood’s equation to be used.

The mean HLL value in our dataset was 1.6 mm, and a maximum value of 3.8 mm was observed. Additionally, CDL_{BM} was observed to be significantly shorter than the CDL_{TIP}. These results indicate that the assumption that the BM reaches the end of the entire cochlea could be clinically consequential. When publishing the function for the cochlear tonotopic map, Greenwood presented the function coefficients specifically for a cochlea with a CDL_{BM} of 35 mm [5]. In order to determine the frequency map for a cochlea with a different CDL_{BM}, the coefficients must be scaled appropriately, as described by Greenwood [5]. Utilizing the mean values determined in this work, we examine the hypothetical case of a cochlea with CDL_{BM} of 39.0 mm and HLL of 1.6 mm. It was found that the assumption that the BM reaches the very apical tip of the cochlea (error of 1.6 mm) could result in a pitch-

mismatch of approximately 280 Hz at an insertion depth of 5 mm, and approximately 120 Hz at an insertion depth of 25 mm. A 120 Hz mismatch at a 25 mm insertion depth (approximately 780 Hz–900 Hz) corresponds to a gap of over two semitones, and this pitch-mismatch can potentially be important for the perception of music, complex speech, and tonal languages [26, 27]. CIs currently have limitations due to their insertion depth and the resolution of electrode stimulation, however this hypothetical situation provides evidence that the size of the helicotrema has a measurable effect on the frequency distribution and perception in individuals. Generalized CI pitch-maps have been reported to result in a pitch-mismatch of over one octave [28, 29], due to variance in cochlear size and difficulties measuring the BM in the helicotrema and hook region. Accurate modelling of the helicotrema has the potential to reduce a portion of this error. The cochlear hook region is another complex portion of the BM that has had limited description previously in the literature. Current measurement protocols in the hook region can also result in CDL errors in the order of 2 mm, and to further reduce CDL errors and consequently pitch-mapping errors, a complete analysis of the cochlear hook region in three-dimensions is required. Tonotopic frequency mismatch is potentially consequential because it is suggested that correct tonotopic stimulation is required for complex-sound perception [30].

The high correlation observed between HLL and HAL measurements indicate a consistent morphological relationship in the helicotrema region. A linear relationship was determined that significantly predicted the HAL of the cochleae based on the HLL, with changes in HLL accounting for over 93% of the variability detected in the HAL. This may imply that cochleae twist in a consistent way in the helicotrema region regardless of their size. This is a valuable preliminary result because it indicates that the apical turns of the cochlea have a predictable behaviour.

Regression analysis additionally revealed a significant relationship between CDL_{TIP} and CDL_{BM} in our sample set. It was observed that CDL_{BM} can be estimated with confidence based on the CDL_{TIP} value using the equation: $CDL_{BM} = 0.88(CDL_{TIP}) + 3.71$. CDL_{BM} is not directly measurable on most clinical and research imaging modalities, however CDL_{TIP} is a parameter that can be estimated using validated published techniques and models [10]. This study, therefore, provides a correction factor to accurately predict the total CDL_{BM} based on CDL_{TIP} . This can be incorporated into various analytical equations already published [10, 13, 18, 25]. Furthermore, the HLL and HAL values presented herein can be used to develop more anatomically accurate numerical models of the human cochlea. Current models have made approximations regarding the size of the helicotrema, and the detailed measurements from this study can be integrated to produce more accurate biomechanical models of the cochlear apex [21, 31].

The sample size in this study was limited by the challenges associated with SR-PCI. SR-PCI was conducted at the Canadian Light Source Inc., a government facility that competitively grants scan time. The synchrotron facility is geographically distant from the home institution of the authors, and access is limited based on the high facility demand. The initial cochlear dataset scanned with SR-PCI was chosen to represent a wide distribution of CDL values and cochlear shapes to maximize representation of the general population. The relationships derived in this study are limited by the small sample size, however they provide statistically strong trends that are expected to relate CDL_{TIP} to CDL_{BM} in patients. Furthermore, measurements in this study were taken at the LW of the cochleae. Previous publications have suggested the organ of Corti length is clinically relevant, and suggest correction factors to relate CDL values at the LW to CDL values at the organ of Corti [32]. These previously published correction factors can be used concurrently with the adjustment presented herein to achieve CDL_{BM} at different locations on the cochlear partition. This was the first study to analyze the length and morphology of the helicotrema and cochlear apex. Future studies will include additional SR-PCI scans of

the helicotrema region with a more dedicated field of view to optimize visualization of anatomic detail. Electron microscope scans of the cochlear apex will be combined with the SR-PCI findings to obtain accurate 3D models of the BM and its supporting structures in the helicotrema region.

Conclusion

Although morphological analyses were previously attempted [2], SR-PCI allowed high-resolution imaging of both the cochlear soft tissues and bony walls in the apex. HLL and HAL values were measured on 14 cadaveric SR-PCI scans, and additionally CDL_{TIP} and CDL_{BM} were determined on a sub-set of six samples. It was determined that a significant relationship exists between HLL and HAL in our sample set, indicating constant morphology in the helicotrema region. A significant relationship was also found between CDL_{BM} and CDL_{TIP} in our sample set. This indicates that CDL_{BM} can be estimated from CDL_{TIP} measurements using the equations presented herein. CDL_{BM} can be subsequently used for more anatomically accurate CI planning and pitch-mapping.

Abbreviations

3D: Three-dimensional; BM: Basilar membrane; CDL: Cochlear duct length; CI: Cochlear implant; HAL: Helicotrema angular length; HLL: Helicotrema linear length; LW: Lateral wall; RW: Round window; SR-PCI: Synchrotron radiation phase-contrast imaging

Acknowledgements

Financial support was provided by the Natural Sciences and Engineering Research Council of Canada and the Province of Ontario.

Authors' contributions

LWH performed image processing, measurements, data analysis, and manuscript preparation. HL performed image processing, generated figures, and reviewed the manuscript. HRA performed anatomical analysis, reviewed the data analysis, and reviewed the manuscript. HML performed the imaging and edited the manuscript. SKA performed anatomical analysis, reviewed data analysis, and edited the manuscript. HML and SKA were primary supervisors for LWH. All authors read and approved the final manuscript.

Funding

HML was supported by a Natural Sciences and Engineering Research Council (NSERC) Discovery Grant. LWH was supported by a NSERC Canada Graduate Scholarship-Masters and a Queen Elizabeth II Graduate Scholarship in Science and Technology.

Availability of data and materials

The datasets analyzed during the current study are available upon reasonable request at the discretion of the authors.

Ethics approval and consent to participate

All cadaveric specimens were obtained with permission from the body bequeathal program at Western University, London, Ontario, Canada in accordance with the Anatomy Act of Ontario and Western's Committee for Cadaveric Use in Research. (Approval Number: 19062014).

Consent for publication

Not applicable.

Competing interests

The authors declare that they have no competing interests.

Author details

¹School of Biomedical Engineering, Western University, London, Ontario, Canada. ²Department of Surgical Sciences, Head and Neck Surgery, Section of Otolaryngology, Uppsala University Hospital, Uppsala, Sweden. ³Department of Otolaryngology, Uppsala University Hospital, Uppsala, Sweden. ⁴Department of Otolaryngology - Head and Neck Surgery, Western University, London, Ontario, Canada. ⁵Department of Medical Biophysics, Western University, London, Ontario, Canada. ⁶Department of Electrical and Computer Engineering, Western University, London, Ontario, Canada.

Received: 2 August 2019 Accepted: 23 December 2019

Published online: 06 January 2020

References

1. Erixon E, Högstorp H, Wadin K, Rask-Andersen H. Variational anatomy of the human cochlea. *Otol Neurotol*. 2009;30(1):14–22.
2. Avci E, Nauwelaers T, Lenarz T, Hamacher V, Kral A. Variations in Microanatomy of the Human Cochlea. *J Comp Neurol Res Syst Neurosci*. 2014;3261:3245–61.
3. Hardy M. The length of the organ of Corti in man. *Am J Anat*. 1938;62(2): 291–311.
4. Koch RW, Ladak HM, Elfarnawany M, Agrawal SK. Measuring Cochlear duct length - a historical analysis of methods and results. *J Otolaryngol Head Neck Surg*. 2017;46(1):1–11.
5. Greenwood DD. A cochlear frequency-position function for several species—29 years later. *J Acoust Soc Am*. 1990;87(6):2592–605.
6. Noble JH, Hedley-Williams AJ, Sunderhaus L, Dawant BM, Labadie RF, Camarata SM, et al. Initial results with image-guided cochlear implant programming in children. *Otol Neurotol*. 2016;37(2):e63–9.
7. Jiam NT, Pearl MS, Carver C, Limb CJ. Flat-panel CT imaging for individualized pitch mapping in cochlear implant users. *Otol Neurotol*. 2016; 37(6):672–9.
8. Jiam NT, Gilbert M, Cooke D, Jiradejvong P, Barrett K, Caldwell M, et al. Association between flat-panel computed tomographic imaging-guided place-pitch mapping and speech and pitch perception in Cochlear implant users. *JAMA Otol Head Neck Surg*. 2018;145(2):109–16.
9. Takagi A, Sando I. Computer-aided three-dimensional reconstruction: a method of measuring temporal bone structures including the length of the cochlea. *Ann Otol Rhinol Laryngol*. 1989;98(7):515–22.
10. Pietsch M, Aguirre Dávila L, Erfurt P, Avci E, Lenarz T, Kral A. Spiral Form of the Human Cochlea Results from Spatial Constraints. *Sci Rep*. 2017;7:7500.
11. Kawano A, Seldon HL, Clark GM. Computer-aided three-dimensional reconstruction in human cochlear maps: measurement of the lengths of organ of corti, outer wall, inner wall, and Rosenthal's canal. *Ann Rhinol Otol Laryngol*. 1996;105(9):701–9.
12. Escudé B, James C, Deguine O, Cochard N, Eter E, Fraysse B. The size of the cochlea and predictions of insertion depth angles for cochlear implant electrodes. *Audiol Neurotol*. 2006;11(SUPPL. 1):27–33.
13. Alexiades G, Dhanasingh A, Jolly C. Method to estimate the complete and two-turn cochlear duct length. *Otol Neurotol*. 2015;36(5):904–7.
14. Würfel W, Lanfermann H, Lenarz T, Majdani O. Cochlear length determination using cone beam computed tomography in a clinical setting. *Hear Res*. 2014;316(April 2007):65–72.
15. Lexow GJ, Kluge M, Gellrich NC, Lenarz T, Majdani O, Rau TS. On the accuracy of cochlear duct length measurement in computed tomographic images. *Eur Arch Otorhinolaryngol*. 2018;275(5):1077–85.
16. Erixon E, Rask-Andersen H. How to predict cochlear length before cochlear implantation surgery. *Acta Otolaryngol*. 2013;133(12):1258–65.
17. Finley CC, Roland PS, Thomas J. Consensus panel on a cochlear coordinate system applicable in histologic, physiologic, and radiologic studies of the human cochlea. *Otol Neurotol*. 2011;31(5):722–30.
18. Koch RW, Elfarnawany M, Zhu N, Ladak HM, Agrawal SK. Evaluation of Cochlear duct length computations using synchrotron radiation phase-contrast imaging. *Otol Neurotol*. 2017;38(6):e92–9.
19. Braun K, Böhnke F, Stark T. Three-dimensional representation of the human cochlea using micro-computed tomography data: presenting an anatomical model for further numerical calculations. *Acta Otolaryngol*. 2012;132(6):603–13.
20. Hilding AC. Studies on the otic labyrinth. VII. The helicotrema. *Ann Otol Rhinol Laryngol*. 1955;64:278–90.
21. Sasmal A, Grosh K. Unified cochlear model for low- and high-frequency mammalian hearing. *Proc Natl Acad Sci*. 2019;116(28):13983–8.

22. Iyer JS, Zhu N, Gasilov S, Ladak HM, Agrawal SK, Stankovic KM. Visualizing the 3D cytoarchitecture of the human cochlea in an intact temporal bone using synchrotron radiation phase contrast imaging. *Biomed Opt Express*. 2018;9(8):3757–67.
23. Elfarnawany M, Alam SR, Rohani SA, Zhu N, Agrawal SK, Ladak HM. Micro-CT versus synchrotron radiation phase contrast imaging of human cochlea. *J Microsc*. 2017;265(3):349–57.
24. Vu TH, Perazzini C, Puechmaile M, Bachy A, Mulliez A, Boyer L, et al. CT-scan contouring technique allows for direct and reliable measurements of the cochlear duct length: implication in cochlear implantation with straight electrode-arrays. *Eur Arch Otorhinolaryngol*. 2019;276(8):2135–40.
25. Schurzig D, Timm ME, Batsoulis C, Salcher R, Sieber D, Jolly C, et al. A Novel Method for Clinical Cochlear Duct Length Estimation toward Patient-Specific Cochlear Implant Selection. *Oto Open*. 2018;2:4.
26. Jiam NT, Limb CJ. Rhythm processing in cochlear implant-mediated music perception. *Ann N Y Acad Sci*. 2019;1453:22–8.
27. Deroche MLD, Lu HP, Kulkarni AM, Caldwell M, Barrett KC, Peng SC, et al. A tonal-language benefit for pitch in normally-hearing and cochlear-implanted children. *Sci Rep*. 2019;9(1):1–12.
28. Peters JPM, Bennink E, Grolman W, van Zanten GA. Electro-acoustic pitch matching experiments in patients with single-sided deafness and a cochlear implant. Is there a need for adjustment of the default frequency allocation tables? *Hear Res*. 2016;342:124–33.
29. Peters JPM, Bennink E, Van Zanten GA. Comparison of place-versus-pitch mismatch between a Perimodiolar and Lateral Wall Cochlear implant electrode Array in patients with single-sided deafness and a Cochlear implant. *Audiol Neurotol*. 2019;24(1):38–48.
30. Oxenham AJ, Bernstein JGW, Penagos H. Correct tonotopic representation is necessary for complex pitch perception. *Proc Natl Acad Sci*. 2004;101(5): 1421–5.
31. Xu LF, Ta N, Rao ZS, Tian J bin. Finite element model of human cochlea considering of the Helicotrema size. *Appl Mech Mater*. 2013;456:576–81.
32. Dhanasingh A. Cochlear duct length along the outer wall vs organ of corti: which one is relevant for the electrode array length selection and frequency mapping using Greenwood function? *World J Otorhinolaryngol - Head Neck Surg*. 2018;5(2):117–21.

Publisher's Note

Springer Nature remains neutral with regard to jurisdictional claims in published maps and institutional affiliations.

Ready to submit your research? Choose BMC and benefit from:

- fast, convenient online submission
- thorough peer review by experienced researchers in your field
- rapid publication on acceptance
- support for research data, including large and complex data types
- gold Open Access which fosters wider collaboration and increased citations
- maximum visibility for your research: over 100M website views per year

At BMC, research is always in progress.

Learn more biomedcentral.com/submissions

